UDK: 621.383.7:621.315.2:517.9
COSATI: 09-03, 17-02

Accurate Modelling of Modern Photonic Devices with Complex Geometries in Transverse Plane and Longitudinal Direction

Dušan Djurdjević, PhD (Eng)[1)]

This paper reviews some key techniques for design of new high performance photonic devices and widely used optoelectronic components. The emphasis of this work is upon numerical simulation techniques for integrated photonics, based on the numerical solution of the 3D vector Helmholtz's equation subject to open boundary conditions. In particular, the focus is on the beam propagation method (BPM) and its most popular variant: the finite difference beam propagation method (FD-BPM). Recently developed co-ordinate transformation approaches, such as the structure-related (SR) FD-BPM, allow the comfortable analysis of a wide variety of geometrically complex photonic structures, especially when the structure under analysis is changing in the longitudinal direction or in the transversal plane, containing oblique or curved dielectric interfaces. The SR-FD-BPM is a particularly attractive modelling tool for the expected complexity of the near-future photonic integrated circuitry (PIC). Some illustrative design examples, based on the efficient co-ordinate transformation and structure related algorithms, are presented in the paper.

Key words: **optoelectronics, photonics, beam propagation, integrated circuits, numerical simulation, finite difference method.**

Introduction

THE amount of applications the photonics industry serves grows, making the photonics market both marvelous and mysterious. Major advances in photonics at the end of the 20th and in the 21st century have been driven by the demands of the telecom and datacom boom, including in large part the growth of the Internet. The light-wave datacom transmission systems; military photonics systems and projects, such as optical guns, REDOWL robots designed to provide gunshot detection, intelligence, surveillance, homeland security and border control to military forces and government agencies; advanced aerospace and navigation systems; household optics devices used into the realm of the consumer – and other developments and new discoveries in this ever-changing industry, make the future of the photonics uncertain. Technologies, which were once reserved for use in scientific and military environments, have entered the non-military market space, finding new consumer-based and more commercial-based applications.

Photonic integrated circuits (PIC) and fiber-optic photonic components are the foundation of aforementioned systems. A move into the consumer market has required manufacturers to increase efficiencies and reduce costs, yet obeying stringent demands to enable production of high-quality components [fibers, lasers, light-emitting diodes, silicon photodiodes, detectors, electro-optic modulators, couplers, optical switches, polarizers, polarization rotators, wavelength-demultiplexing devices (WDM's), etc.].

Less apparent to wider audience, however playing the crucial and extremely significant role behind the military, industrial and commercial scene, have been the developments and the research in modelling techniques and design of commercialized computer-aided design (CAD) softwares for modelling photonic and opto-electronic components and systems. The commercial success of photonics is strongly dependent upon the used design methodologies and tools.

The most of photonics devices and components are built in dielectric waveguide technology. Basically, optical modes can propagate in a given, uniform cross-section of a waveguiding structure. Most photonic devices, however, change their shape in the direction of propagation. The light propagation computer simulation in such cases provides an excellent means of achieving results in this serious design issue. Producing computer simulation techniques and software for photonic and optoelectronic design is a highly specialized area, requiring knowledge, understanding and experience in the underlying physical process involved, numerical techniques, software engineering and project management. The beam propagation method (BPM) is, certainly, the most widely used numerical simulation technique for modeling photonic devices, and most commercial software for such modeling is based on it. The BPM is essentially a particular approach to numerical solving of appropriate approximation of the exact vector Helmholtz's equation for monochromatic waves. Several BPM algorithms have been developed in recent two decades (FE-BPM, MoL-BPM, FDTD-BPM, etc.), however, one of the most commonly used simulation algorithm in integrated optics is the frequency-domain based finite difference beam propagation method (FD-BPM), [1-5].

The research attention in the earlier FD-BPM approaches has been given to improving numerical techniques for solving large sparse matrix equations involved in the method. Recent focus in FD-BPM research and design has

[1)] Faculty Technical Scientific, Knjaza Miloša 7, 38220 Kosovska Mitrovica, SERBIA

been moved on developing improved FD schemes with more accurate treatment of the dielectric interfaces between the dielectric regions of waveguide based structures, see for example [6]. The emphasis on the improved FD formulas stands because the standard implementation of the FD-BPM in a rectangular co-ordinate system causes serious problems and certain restrictions if the structure under analysis contains oblique or curved interfaces in the transverse plane. The source of these restrictions is the inevitable staircase approximation of the boundaries which occurs during the finite difference discretization procedure (Fig.1). Improved FD schemes provide true accuracy of the second order $O\left(\Delta^2\right)$, where Δ denotes the transverse step size, for the structures with a constant cross-section in the transverse plane, regardless of the placement of the dielectric interface in the structure. Another successful approach is the use of the co-ordinate transformation methods, see for example [7], such as the structure related (SR) FD-BPM, [8-10]. The SR schemes eliminate non-physical scattering, yielding significant reduction in computational requirements. The SR co-ordinate systems, such as tapered, oblique, bi-oblique co-ordinate systems, naturally follow the local geometry of the structure under analysis.

When the waveguide based structure is changing in the longitudinal direction of the propagation, the FD-BPM reformulation in non-orthogonal, structure related co-ordinate systems successfully remedies the deficiency of the standard rectangular FD schemes, [11-15]. Some new, promising approaches have been recently proposed in [16-17], featuring the separation of the BPM propagation algorithm from the discretization FD grid.

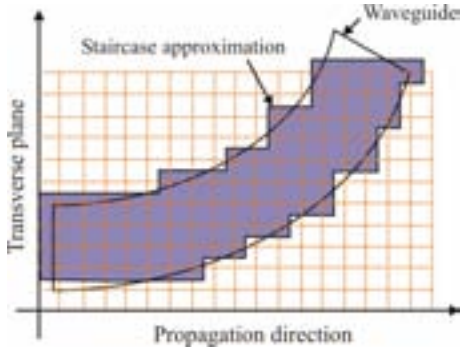

Figure 1. Staircase approximation on the curved waveguide forced onto a Cartesian grid, causes non-physical numerical noise in simulation. Reducing these errors by denser sampling usually results in much longer simulation times.

The goal of the paper is to review the range of the applicability of the recently developed structure related beam propagation methodology as well as to emphasize some illustrative results. The author has been a member of the Nottingham's Electromagnetics Research Group for several years (2001-2004), presently the George Green's Institute, as a part of the City University of Nottingham, United Kingdom, which has contributed to those major advances in numerical simulation techniques in photonics, [1, 2, 9, 10, 13, 14, 15].

Structure related FD-BPM in the transverse plane

The improved FD approach takes into account the boundary conditions for the field and its derivatives near the dielectric interfaces, which results in second order accurate formulas. However, the FD-BPM can be extended to non-orthogonal structure-related transverse co-ordinate systems, where oblique boundaries can be modelled exactly.

The Nottingham's research team have pioneered the use of structure related co-ordinate schemes for FD-BPM, where the discetrization procedure exactly matches the local geometry of the structure, thus eliminating non-physical scattering due to the staircasing effect. The resulting SR FD-BPM algorithm allows simulations with noticeably reduced numerical noise and shortened simulation time. The advantage of this approach is that, in comparison to the standard rectangular schemes, coarser mesh sizes can be used for the same accuracy offering a significant reduction in computational time involved. The non-orthogonal co-ordinate FD-BPM has been applied to the analysis of structures with oblique, bi-oblique, tapered, and tapered-oblique [8-11] cross-sections in the transverse plane. The general theory of the structure-related (SR) non-orthogonal co-ordinate systems was given in [12].

As an example of the SR FD-BPM approach, some results of the sloped walled rib waveguide analysis are given, see Fig.2. The details can be found in [9,10].

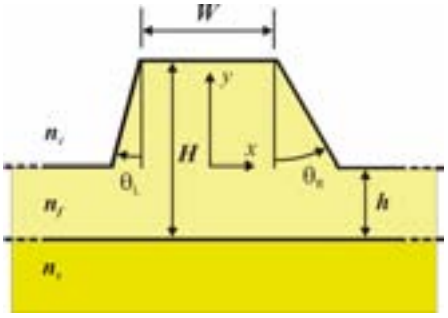

Figure 2. The transverse cross-section profile of a rib waveguide with sloped walls.

The transverse $x-y$ plane is transformed by the combination of two non-orthogonal co-ordinate systems: oblique and tapered, coupled with the rectangular one (scheme: "ROTOR" – **r**ectangular-**o**blique-**t**apered-**o**blique-**r**ectangular).

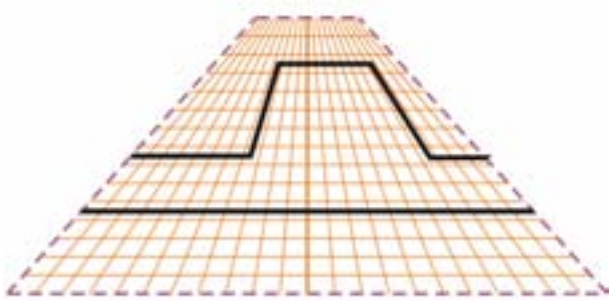

Figure 3. Discretization of the rib waveguide cross-section given in Fig.2, by using the tapered FD mesh, [9].

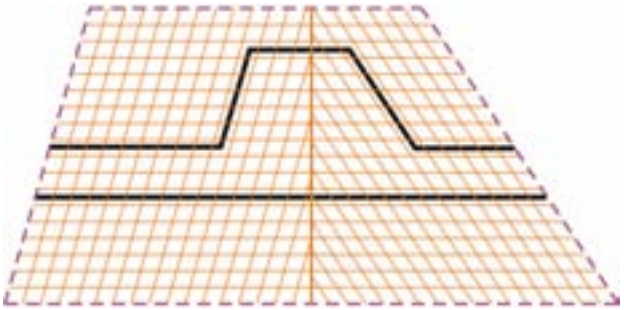

Figure 4. Discretization of the rib waveguide cross-section given in Fig.2, by using the bi-oblique FD mesh, [9].

The examples of: the tapered FD mashing are shown in Fig.3, bi-oblique FD mashing in Fig.4, and the "ROTOR" mashing is shown in Fig.5. The sloped walled rib waveguide and similar structures are fabricated and used in photonic integrated circuits as single section passive polarization rotators, [18].

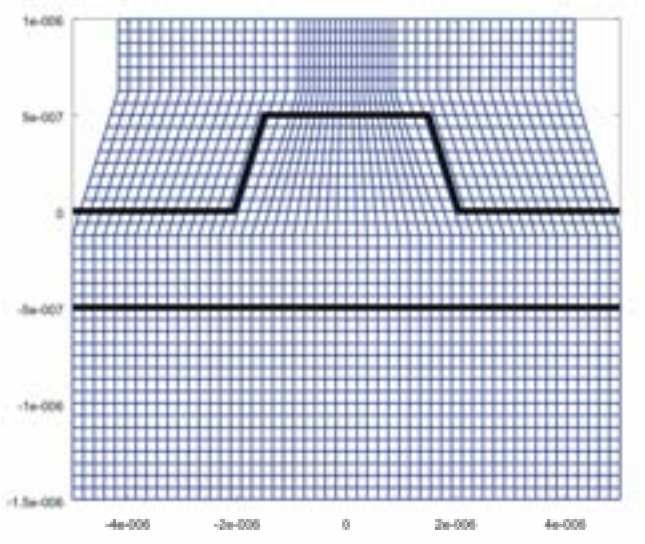

Figure 5. Discretization of the rib waveguide with cross-section given in Fig.2, by using the "ROTOR" – FD mesh, [10].

To verify the validity of the SR approach, the simplest case of the paraxial scalar three-dimensional Helmholtz's equation is derived in the oblique and tapered non-orthogonal transverse co-ordinate systems. The scalar Helmholtz's equation in the rectangular co-ordinate system x, y and z, reads

$$\left[\frac{\partial^2}{\partial x^2}+\frac{\partial^2}{\partial y^2}+\frac{\partial^2}{\partial z^2}+k_0^2 n^2(x,y)\right]\varphi(x,y,z)=0, \qquad (1)$$

where $k_0 = 2\pi/\lambda_0$ is the free space wave number, λ_0 is the operating wavelength, $n(x,y)$ is the z invariant refractive index and $\varphi(x,y,z)$ represents the scalar electric or magnetic field. eq.(1) is not suitable for obtaining stable numerical algorithms and it is usually replaced with its first order paraxial approximation by assuming a slowly-varying envelope approximation of the field

$$\varphi(x,y,z)=\phi(x,y,z)e^{-j\beta z}, \qquad (2)$$

where $\beta = k_0 n_0$ is an imposed propagation constant for the scalar field envelope φ. By neglecting the $\partial^2/\partial z^2$ term, the one-way paraxial wave equation, or Fresnel's equation, is obtained,

$$j2k_0 n_0\frac{\partial\phi}{\partial z}=\frac{\partial^2\phi}{\partial x^2}+\frac{\partial^2\phi}{\partial y^2}+k_0^2\left(n^2-n_0^2\right)\phi, \qquad (3)$$

where n_0 denotes a reference refractive index. The wave equation (3) is derived in the Cartesian orthogonal transverse co-ordinate system (x,y). However, eq.(3) can be rewritten in any orthogonal or non-orthogonal transverse co-ordinate system. If we choose the non-orthogonal oblique co-ordinate system (u,v), in the transverse plane, in which $u = x \mp y\tan\theta$, $v = y$, and

$$\frac{\partial}{\partial u}=\frac{\partial}{\partial x},\quad \frac{\partial}{\partial v}=\frac{\partial}{\partial y}\mp\tan\theta\frac{\partial}{\partial x}, \qquad (4)$$

one can derive the scalar paraxial wave equation in the oblique co-ordinate system as:

$$\sigma\frac{\partial\phi}{\partial z}=\sec^2\theta\frac{\partial^2\phi}{\partial u^2}\pm 2\tan\theta\frac{\partial^2\phi}{\partial u\partial v}+\frac{\partial^2\phi}{\partial v^2}+\kappa^2\phi, \qquad (5)$$

where $\sigma = jk_0 n_0$, $\kappa^2 = k_0^2\left(n^2-n_0^2\right)$ and the envelope of the field $\phi=\phi(u,v,z)$ and the refractive index $n=n(u,v)$ are functions of the oblique co-ordinates u and v. In Eqs. (4) and (5) the sign "+" stands for the right-hand side and "-" for the left-hand side of the oblique co-ordinate system, see Fig.6.

Similarly, in the case of a tapered co-ordinate system (t,v) in the transverse cross-section, see Fig.6, in which $t=\tan\theta$, $x=t(y-y_{OR})$, $v=y$, and

$$\frac{\partial}{\partial x}=\frac{1}{v-v_0}\frac{\partial}{\partial t},\quad \frac{\partial}{\partial y}=\frac{\partial}{\partial v}-\frac{t}{v-v_0}\frac{\partial}{\partial t}, \qquad (6)$$

the scalar paraxial wave equation can be expressed as:

$$\sigma\frac{\partial\phi}{\partial z}=\frac{\partial^2\phi}{\partial v^2}-\frac{2t}{v-v_0}\frac{\partial^2\phi}{\partial v\partial t}+\frac{1}{(v-v_0)^2}\frac{\partial}{\partial t}\left[\left(1+t^2\right)\frac{\partial\phi}{\partial t}\right]+\kappa^2\phi. \qquad (7)$$

Thus, the envelope of the scalar field $\phi=\phi(t,v,z)$ and the refractive index $n=n(t,v)$ are the functions of the tapered co-ordinates t and v. In equations (6) and (7) the origin of the tapered co-ordinate system (x_0,y_0) is given parametrically as $v_0 = y_0 = x_0\cot\theta$. The right-hand side case is shown in Fig.6.

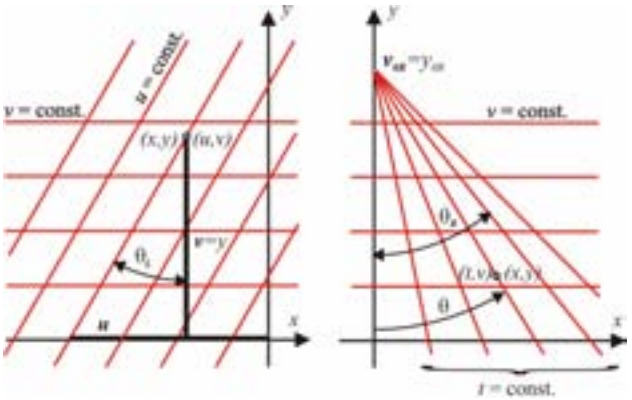

Left hand side **oblique** c.s Right hand sided **tapered** c.s.

Figure 6. Left-hand sided oblique and right-hand sided tapered non-orthogonal transverse co-ordinate systems. The angles θ_L and θ_R are measured with respect to negative direction of the y axis.

The transverse plane (i.e. the transverse computational window) can be discretized by using a few approaches: 1) to use a (t,v) plane and solve the problem completely in the tapered co-ordinate system, Figures 3 and 2) to use only the bi-oblique co-ordinate system and to present the computational area in the (u,v) plane, Fig.4, or Fig.3) to use a combination of two non-orthogonal co-ordinate systems: oblique and tapered, coupled with a rectangular, as shown in Fig.5. In Figures 3 and 4 the FD disctretizing mesh is clearly emphasized and the dashed lines outline the

computational window. There is no best method for obtaining the FD mesh, because each discretization scheme offers potential benefits. In the Rectangular-Oblique-Taper-Oblique-Rectangular ("ROTOR") scheme, Fig.5, used in this simulation example, rectangular, oblique and tapered co-ordinate systems are utilized together, sharing the common co-ordinate variable *y*. The Hadley's transparent boundary conditions (TBC), [19], are employed at the edges of the computational window. This scheme serves as a good example of how to combine rectangular with other non-orthogonal co-ordinate systems with retaining greatly improved accuracy. However, the intrinsic deficiency of the ROTOR-like discretizing schemes is the necessity to join different orthogonal and non-orthogonal systems, which can potentially complicate the algorithm. The co-ordinate merging can be done, for example, in a very satisfactory way, by using a simple linear approximation, see [9] for details.

With the co-ordinate systems chosen and adapted to the structure to be analyzed and the FD discretizing scheme of the computational area determined, an SR FD-BPM algorithm can be easily developed. For solving the propagation constant of the fundamental scalar mode, the imaginary-distance propagation method in a longitudinally invariant waveguide is adopted, [20], and a standard Crank-Nicolson method and iterative solver is used. Although for a real and precise solution of the polarization rotator problem a fully-vectorial approach is required, the present analysis shows that even in the simplest case of the scalar wave equation approximation, a significant gain in calculation efficiency can be achieved, in comparison to the standard rectangular FD-BPM algorithms.

The structure related ROTOR FD-BPM and the standard rectangular FD-BPM algorithm have been applied to a low-index contrast symmetric sloped sided rib waveguide, cross-section shown in Fig.3, to estimate the efficiency of the novel algorithm. The operating wavelength is $\lambda_0 = 1.55$ μm m, the dimensions of the structure studied are, in the notation of the Fig.3, W=2 μm, H=1.5 μm, h=0.4 μm, $\theta_L = \theta_R = 25^\circ$, and the refractive indices of the rib core, substrate and cladding are n_f=3.44, n_s=3.40 and n_c=3.40 respectively. By using a very fine transverse mesh $(\Delta x = \Delta y = \Delta = 0.01\ \mu\text{m})$ rectangular and SR ROTOR co-ordinate algorithms converged to a six significant digit value for the effective index, n_{eff}=3.42009. However, the superior computational efficiency shows the SR ROTOR FD-BPM scheme: the same degree of the relative error is achieved for $\Delta \cong 0.1\ \mu\text{m}$ in the SR ROTOR FD-BPM analysis, and $\Delta \cong 0.06\ \mu\text{m}$ in the standard rectangular FD-BPM analysis. In the ROTOR scheme Δ refers to the discretization in the lower rectangular area. The use of the novel structure related scheme gives results with the same order of accuracy with at least a factor of 10 better CPU time/memory performance in comparison to the standard rectangular scheme in the low-index contrast case (the factor is greater in the weakly-guiding cases) and at least a factor of 3 in the strong-guiding case.

Fig.7 compares the fields obtained by the SR ROTOR and the standard rectangular FD-BPM in the strong-guiding example structure. In both simulations $\Delta x = \Delta y = 0.1\ \mu\text{m}$ has been adopted. At z=0 a Gaussian beam has been launched and propagated to the distance of 500 μm with the propagation step $\Delta z = 1\ \mu\text{m}$. It can be seen how the staircasing numerical noise sourced around the oblique boundaries deteriorates the standard rectangular FD-BPM simulation. The numerical noise increases with z, and as a result, the field beam is spreading and gives a wrong simulation output. The field plots obtained via the SR ROTOR algorithm (simulations and plotting parameters are kept the same) show that the numerical noise is reduced, which consequently enables a more accurate simulation.

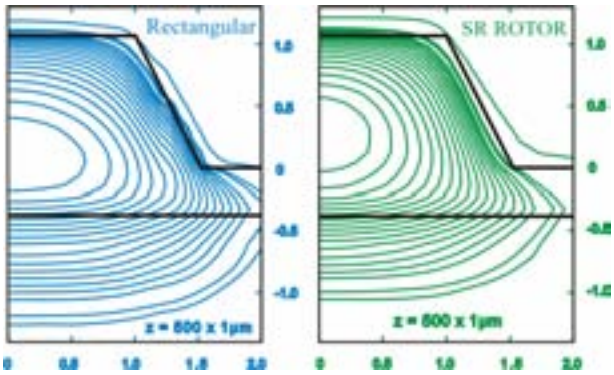

Figure 7. The field plots obtained with the standard rectangular FD-BPM (left-hand side plot) and the SR ROTOR FD-BPM (right-hand side plot) simulation. The contours of the field are plotted with the 0.05 log increment (from 10^0, $10^{-0.05}$, $10^{-0.1}$, up to 10^{-1}) of the field maximum.

In general, the results obtained for the modal propagation constant and the BPM field simulations of the sloped sided rib waveguide confirm that the extended method yields substantial advantages in comparison to the standard rectangular co-ordinate system based algorithms. An SR FD-BPM algorithm allows considerable relaxing of the mesh size to obtain results to a prescribed accuracy with coarser meshes, thereby offering savings in both computational time and memory.

Structure related FD-BPMin the longitudinal direction

When the waveguide under analysis changes in the direction of the propagation, SR co-ordinate systems successfully remedy the staircasing involved in the standard rectangular FD schemes. The 2D examples of the propagation in the tapered and in the oblique non-orthogonal co-ordinates are shown in Figures 8 and 9 respectively.

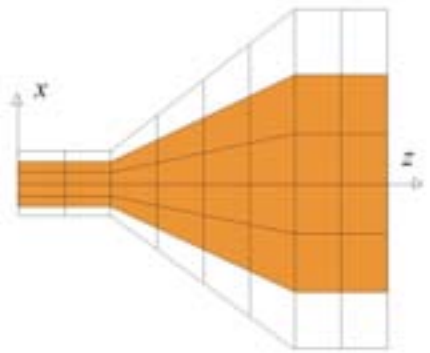

Figure 8. The 2D example of the "tapered" propagation, [11].

The SR-BPM approach and the resulting algorithm are used nowadays to design tapered, oblique and bi-oblique shaped optoelectronic waveguides and waveguide-based devices, such as z-variant directional waveguide couplers, y-branches, optical interconnects, waveguide polarizers and similar PIC components that include waveguide bends.

Some illustrative examples and results are given in the present paper, involving a paraxial, semi-vectorial 3D SR-BPM analysis of "S"-curved directional waveguide couplers, together with the comparison with results from a similar standard analysis using a rectangular co-ordinate system. The comparison of the results for the same order of discretization shows the distinct advantages of the SR schemes and the SR-BPM algorithm: the propagation error is reduced and the simulation time is shortened, particularly in 3D simulations.

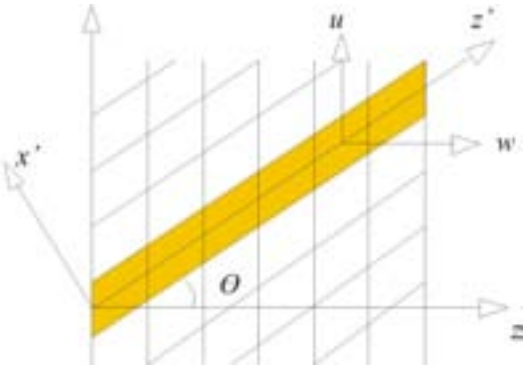

Figure 9. The 2D example of the propagation in the oblique non-orthogonal co-ordinates.

The basic approach of the longitudinally dependent SR-BPM is illustrated by formulating the scalar and semi-vectorial (polarized) SR-BPM wave-equation. Under the assumption that the refractive index $n(x,y,z)$ at the operating wavelength λ_0 varies slowly along the propagation direction z, one can derive the so-called semi-vectorial Helmholtz's wave equation based on the transverse electric field $E_t = E_t(x,y,z)$, or the transverse magnetic field $H_t = H_t(x,y,z)$,

$$\nabla^2 \Phi_t + n^2 k^2 \Phi_t = 0\,, \tag{8}$$

where k is the local wave number, $k = k_0 n$, $k_0 = 2\pi/\lambda_0$ is the free space wave number, Φ_t can be either E_t or H_t. If, in the general 3D non-orthogonal co-ordinate system (u,v,w) we choose the co-ordinates (u,w) as $x = f(u,w)$, $z = w$ and $y = v$, we obtain the SR wave equation, [12, 14],

$$\left[A\frac{\partial^2}{\partial u^2} - B\frac{\partial^2}{\partial w \partial u} + C\left(k^2 + \frac{\partial^2}{\partial w^2}\right) - D\frac{\partial}{\partial u} + \frac{\partial^2}{\partial y^2} \right] \Phi_t = 0\,, \tag{9}$$

where $\Phi_t = \Phi_t(u,y,w)$ can be either $E_t = E_t(u,y,w)$ or $H_t = H_t(u,y,w)$. The first and second derivatives in (9) with respect to the non-orthogonal transverse plane co-ordinate u and the second derivatives with respect to the standard co-ordinate y are considered to be discontinuous at the boundaries, and $A = A(u,w)$, $B = B(u,w)$, $C = C(u,w)$, $D = D(u,w)$ are functions of the partial derivatives of $f(u,w)$, [12]

$$A = 1 + \left(\frac{\partial f}{\partial w}\right)^2,\quad B = 2\left(\frac{\partial f}{fu}\right)\left(\frac{\partial f}{\partial w}\right),\quad C = \left(\frac{\partial f}{\partial u}\right)^2$$

$$D = \frac{1}{\dfrac{\partial f}{\partial u}}\left[A\frac{\partial^2 f}{\partial u^2} - B\frac{\partial^2 f}{\partial w \partial u} + C\frac{\partial^2 f}{\partial w^2} \right]$$

The propagation is assumed to be in the + u (i.e. the + z with standard rectangular co-ordinate) direction and the field is separated as a slowly-varying envelope function F_t and a fast-oscillating exponential phase term,

$$\Phi_t(u,v,w) = F_t(u,y,w)\,e^{-j\beta w}\,, \tag{10}$$

with β an imposed background propagation constant which has to be determined. By substituting of (10) in (9) and ignoring the $\partial^2/\partial w^2$ term, the paraxial one-way wave equation in the 3D non-orthogonal co-ordinate system (u,y,w) can be derived as,

$$L\frac{\partial}{\partial w}F_t = MF_t\,, \tag{11}$$

where the operators L and M are shown to be [9],

$$L = 2j\beta C + B\frac{\partial}{\partial u}\,, \tag{12}$$

$$M = A\frac{\partial^2}{\partial u^2} + (Bj\beta - D)\frac{\partial}{\partial u} + C\left(k^2 - \beta^2\right) + \frac{\partial^2}{\partial y^2}\,. \tag{13}$$

Eqs (9-11) are derived under the scalar approximation of the field, but they can be straightforwardly upgraded to a semi-vectorial BPM algorithm. The semi-vectorial SR approach can be applied for the desired function $x = f(u,w)$ assuming that propagation occurs in the w direction.

A standard Crank-Nicolson method is easily introduced in the 3D SR-BPM algorithm. For the well confined waveguide fields transparent boundary conditions (TBC), [19], are typically used at the edges of the computational window, otherwise the Berenger's perfectly matched layers (PML) have to be introduced in the algorithm.

3D simulation results

FD-BPM methods have been extensively used in the analysis of bent and curved waveguide based photonics devices. The SR approach allows a designer the flexibility and comfortable analysis of not only the circular-like bends and curvatures. A designer has freedom of choice to use any curvature function providing optimal integrated optic requirements, such as to achieve compact low loss of optoelectronic circuits.

Some illustrative examples of 3D curved directional couplers designs are presented to highlight the effectiveness and flexibility of the SR FD-BPM. The propagation of the fundamental TE and TM modes, with both E- and H-field formulations, are studied and the results compared with those obtained from the simulations based on a rectangular co-ordinate system. The method can be straightforwardly applied to even more complex structures with curved sections.

Waveguide directional couplers exchange the power between guided modes of adjacent waveguides and perform a number of useful functions in optoelectronic circuits, such as power division, switching and modulation. The "S" curved couplers analysed have advantage over couplers

produced from straight segments because of their lower loss properties. Fig.10 shows a symmetrical coupler made from two identical and adjacent but spatially separated curved input and output waveguides and it is used for total power transfer from the input to the output guide. The asymmetrical coupler configuration is shown respectively in Fig.11. In general, one or more curved coupled waveguides with different curvatures and different cross-sections can be considered.

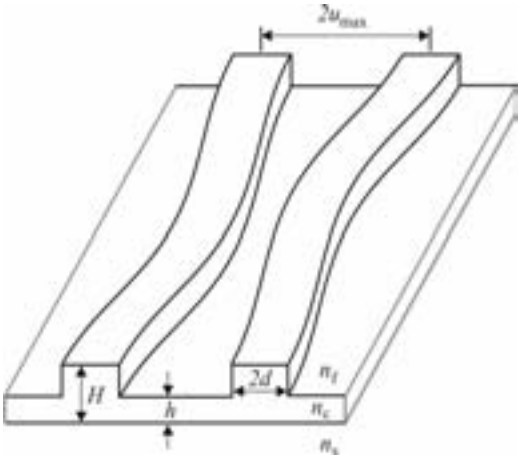

Figure 10. Geometry of 3D directional waveguide coupler in the SR co-ordinate system, (u,w) plane.

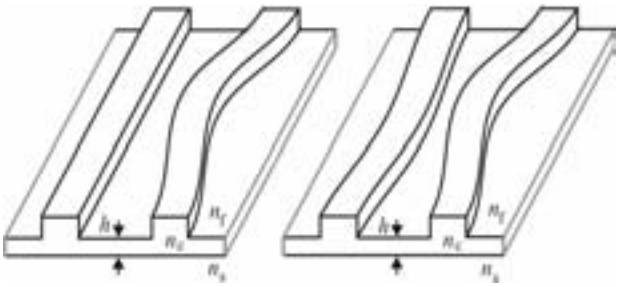

Figure 11. The asymmetrical waveguide coupler diagrams. The coupler is modeled with a straight and curved guide (on the left), or with guides of different curvatures (on the right).

The curve function of an "S" curved coupler can be given parametrically. Amongst various possibilities, for the sake of simplicity, in the proceeding simulation example a cosine type structure related geometry was considered (for $x>0$; symmetrically for $x<0$),

$$x = f(u,v) = u - U_m\left(1-\cos\frac{2\pi w}{L_c}\right), \qquad (14)$$

for $u \ge u_0$ and

$$x = f(u,v) = \frac{u}{u_0}\left[u_0 - U_m\left(1-\cos\frac{2\pi w}{L_c}\right)\right], \qquad (15)$$

for $u \le u_0$, where $U_m = (u_{\max} - u_{\min})/2$, coupler configuration and geometry shown in Fig.12. The functions *A*, *B*, *C* and *D* can be easily obtained analytically, or can be even computed numerically. If the curvature function changes slowly with w, only the function C varies as the square of the gradient of $f(u,w)$ with respect to the oblique co-ordinate u, and if the condition $(w_{\max} - w_{\min}) \ll L_c$ is fulfilled, we can introduce $A \cong 1$, $B \cong 0$, $D \cong 0$, which is always the case except for the sharp guide bends. The discretization mesh, in the (u,w) plane, Fig.12, in the y direction is performed in the standard rectangular manner. The meshing in the u direction follows the curved geometry of waveguides. Around the waveguides the $u = const$. lines are "parallel" to the dielectric boundaries enabling the efficient equally distributed discretization. In the region between the guides, $-u_0 > u > +u_0$, the mesh density can be performed with a noticeably high degree of freedom, with no significant influence on the accuracy of the simulation results.

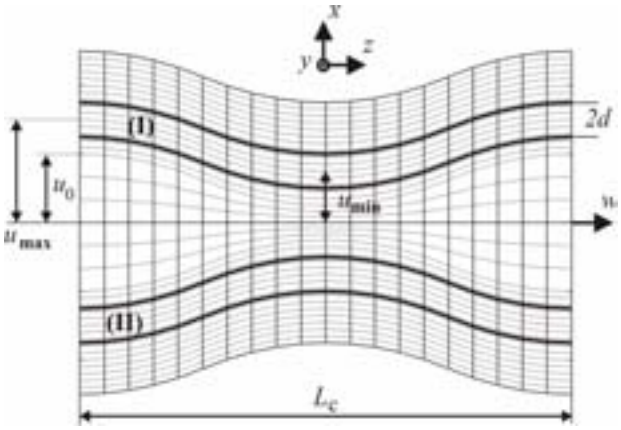

Figure 12. Configuration and geometry of a 3D symmetrical rib waveguide coupler in the SR co-ordinate system, (u,w) plane.

In the performed 3D simulations, the waveguide (I) is considered as an input and the waveguide (II) as an output guide, which can be interchanged because of the symmetry. At $z=0$ the TE or TM mode field is launched from the accurate mode solver in the waveguide (I). The geometry of the coupler guides is kept constant. The total coupling length L_c has to be determined with numerical simulations, under the condition of total power transfer of guided fundamental TE or TM mode from the input (I) to the output (II) mode. The total coupling length L_c is calculated with both rectangular and SR based FD-BPM algorithms, with a standard rectangular one using a very fine mesh and small steps. Both algorithms tend to give the same answer for L_c. The numerical accuracy of the standard and the SR-BPM simulation is evaluated in terms of mode mismatch loss L_M, defined in the 3D case as

$$L_M = 10\log\frac{\left|\int E_i E_c^* dudy\right|^2}{\left[\int |E_i|^2 dudy\right]^2}\ [\text{dB}], \qquad (16)$$

where E_i is the incident fundamental mode at $w=0$ within guide (I) and E_c is the coupled propagation field in guide (II) at $w = L_c$ obtained using the BPM simulation.

A 3D symmetrical rib waveguide coupler of type (14-15), see the inset in Fig.13, and with the (u,w) plane defined as in Fig.12, has been numerically analyzed, and gathered data readily indicate the efficiency and accuracy of the SR approach. Rib waveguides have the identical cross-sections with $n_f = 1$, $n_c = 3.44$, $n_s = 3.4$, $H = 1\ \mu\text{m}$, $h = 0.5\ \mu\text{m}$, $2d = 3\ \mu\text{m}$, $\lambda = 1.15\ \mu\text{m}$. The

total coupling of the fundamental TE mode $(n_{refTE} = 3.41313)$ is obtained with $u_{\max} = 3.0$ μm, $u_{\min} = 1.8$ μm and the total coupling length $L_{cTE} = 4826$ μm. For TM-mode $L_{cTM} = 4769$ μm is obtained. The L_M error in TM-mode propagation as function of the transverse mesh sampling is shown in Fig.13. It is obvious again that the SR scheme enables more accurate 3D simulations of the total coupling. In the SR scheme the number of co-ordinate lines in the coupling region can be relaxed, the index mapping and FD improved formulas coefficients are calculated only once at $z = 0$, consequently giving considerably shorter simulation time for the same order of accuracy in comparison to the rectangular scheme. Both TE- and TM-mode propagation algorithms exhibit almost identical behaviour in terms of accuracy, only the total coupling lengths are different, which is due to the different background propagation constants.

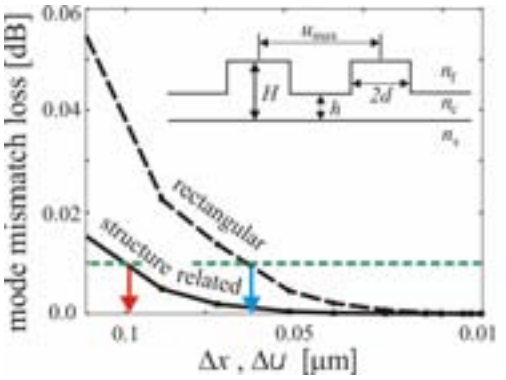

Figure 13. Mode mismatch loss at $w = L_c$ versus the mesh size, TM propagation, for the 3D coupler in the inset of the figure.

The Fig.14 shows the total power coupling of the fundamental TE mode H-field within the symmetrical coupler. The transverse mesh size was kept to be $\Delta x = \Delta y = 0.1$ μm with 600 steps in the w propagation direction. The outer H-field contour in Fig.14 is just 1% of the maximum coupler field, the close one is 5% of the maximum field, and others show 10% field increments. The H-fields in every -slice are normalised to the maximum field. It is obvious from Fig.14, that the almost complete power transfer occurs in the coupler region where rib waveguides are closest to each other.

Due to the unconditionally stable Crank-Nicolson procedure which was used in the algorithm, the longitudinal step size Δw does not affect significantly the accuracy of the simulation. In the 3D example described above, while the transverse mesh size is of the order 0.1 μm and less, very accurate simulations have been obtained with Δw of the order 10 μm. Also, various parametric curves were used in discretizing the region between two coupled guides, with uniform and non-uniform spacing. The analysis of the results shows that the accuracy of simulations is affected significantly, measured in terms of mode mismatch loss L_M, only when the grid redistribution is performed near boundaries. This leads to the conclusion that the accuracy of the BPM simulations depends strongly and mostly on the method used for the discretization of the boundaries region of the waveguide.

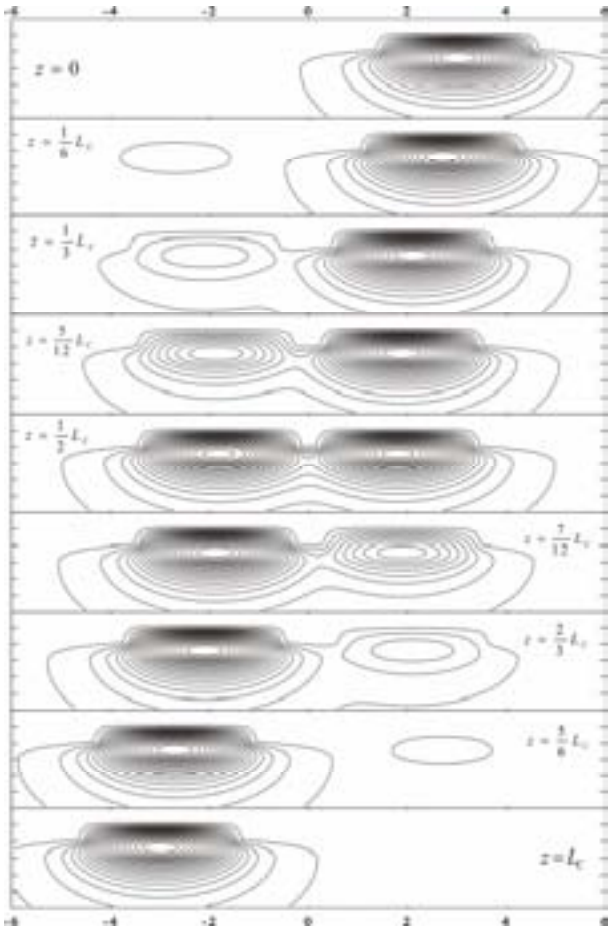

Figure 14. The evolution of the total power transfer of the TE mode H-field during the propagation in a 3D coupler.

The full-vectorial SR BPM version of the algorithm is time-consuming, However, the results do not differ significantly from the results obtained for the same meshes and under the same parameters as in simulations under the semi-vectorial approximation. This leads to the conclusion that in the analysis of the coupling in the curved but with rectangular cross-section waveguide couplers within a millimetre coupling length range a full-vectorial approach is not mandatory.

Conclusion

In this paper, the features of the recently developed co-ordinate transformation based structure related (SR) beam propagation method (BPM) have been addressed and reviewed. With the SR based method the local structure geometry is modelled exactly, either in the transverse plane or in the propagation direction. The numerical simulations, based on an efficient SR finite difference (FD) -BPM algorithm, have been carried out to analyse the z invariant sloped wall rib waveguide and the propagation in 3D curved directional couplers. The results, in both cases, compared with those obtained from the simulations based on a rectangular co-ordinate sysstem, demonstrate the advantages and generality of the SR over the standard rectangular approach, confirming the accuracy and high efficiency of the SR algorithm. The SR-FD-BPM method offers savings in both computational time and memory, enabling flexibility in design of geometrically complex structures with curved sections.

References

[1] BENSON,T.M., DJURDJEVIĆ,D.Z., VUKOVIĆ,A., SEWELL,P.: *Towards Numerical Vector Helmholtz Solutions in Integrated Photonics*, (Invited paper), In: Proc. IEEE on Transparent Optical Networks, 2003, Vol.2, pp.1-4.

[2] BENSON,T.M., SEWELL,P., VUKOVIĆ,A., DJURDJEVIĆ,D.Z.: *Advances in the finite difference beam propagation method*, (Invited paper), In: Proc. IEEE on Transparent Optical Networks, Cracow, Poland,2001, Vol.2, pp.36-41.

[3] SCARMOZZINO,R., GOPINATH,S.A., PREGLA,R., HELFERT,S.: *Numerical Techniques for Modeling Guided-Wave Photonic Devices*, IEEE J. of Sel. Top. In Quant. Electr., 2000, Vol.6, No.1, pp.150-162.

[4] XU,C.L., HUANG,W.P.: *Finite-Difference Beam Propagation Method for Guide-Wave Optics*, Progress In Electromagnetics Research, PIER 11, 1995, pp.1-49.

[5] XU,C.L., HUANG,W.P., STERN and CHAUDHURI,S.K.: *Full-vectorial mode calculations by finite difference method*, IEE Proc.-Optoelectron., 1994, Vol.141, No.5, pp.281-286.

[6] CHIOU,Y.P., CHIANG,Y.C., CHANG,H.C.: *Improved three-point formulas considering the interface conditions in the finite-difference analysis of step-index optical devices*, J. of Lightw. Technology, 2002, Vol.18, No.2, pp.243-251.

[7] YAMAUCHI,J., SHIBAYAMA,J., NAKANO,H.: *Finite-difference beam propagation method using the oblique coordinate system*, Electr. and Communic. in Japan, Part 2, 1995, Vol.78, No.6, pp.740-745.

[8] SEWELL,P., BENSON,T.M., KENDALL,P.C., ANADA,T.: *Tapered beam propagation*, Electronic Letters, 1996, Vol.32, No.11, pp.1025-1026.

[9] DJURDJEVIĆ,D.Z., SEWELL,P., BENSON,T.M., VUKOVIĆ,A.: *Highly efficient finite-difference schemes for structures of nonrectangular cross-section*, Microwave and Opt. Techn. Letters, May 2002, Vol.33, No.6, pp.401-407.

[10] DJURDJEVIĆ,D.Z., SEWELL,P., BENSON,T.M., VUKOVIĆ,A.: *Design of photonics structures with non-orthogonal cross-sections using structure-related finite difference methods*, In: SIOE'02, Cardiff, Wales, 2002.

[11] SUJECKI,S., SEWELL,P., BENSON,T.M., KENDALL,P.C.: *Novel beam propagation algorithms for tapered optical structures*, J. of Lightw. Technology, 1999, Vol.17, No.11, pp.2379-2388.

[12] BENSON,T.M., SEWELL,P., SUJECKI,S., KENDALL,P.C.: *Structure related beam propagation*, Optical and Quantum Electronics, 31, 1999, pp.689-703.

[13] DJURDJEVIĆ,D.Z., BENSON,T.M., SEWELL,P., VUKOVIĆ,A.: *3D analysis of waveguide couplers using a structure related beam propagation algorithm*, In: Proc. OSA/IEEE Integrated Photonics Research Techn. Digest, Washington D.C, USA, 2003, pp.137-139.

[14] DJURDJEVIĆ,D.Z., BENSON,T.M., SEWELL,P., VUKOVIĆ,A.: *Fast and accurate numerical analysis of 3D curved waveguide couplers*, J. of Lightw. Technology, October 2004, Vol.22, No.10, pp.2333-2340.

[15] SEWELL,P., BENSON,T.M., VUKOVIĆ,A., DJURDJEVIĆ,D.Z., WYKES,J.G.: *Computational issues in the simulation of reflective interactions in integrated photonic components*, (Invited paper), In: Proc PIER Symposium, 2004, Pisa, Italy.

[16] HADLEY,G.R.: *Slanted-wall beam propagation*, J. of Lightw. Technology, 2007, Vol.25, No.9, pp.2367-2375.

[17] HADLEY,G.R.: *Beam propagation for tapered wave-guides*, In: Proc. PIER Symposium, Cambridge, USA, 2008.

[18] HUANG,J.Z., SCARMOZZINO,R., NAGY,G., STEEL,M.J., OSGOOD,RM.: *Realization of a Compact and Single-Mode Optical Passive Polarization Converter*, IEEE Photonics Techn. Letters, Mar. 2000, Vol.12, No.3, pp.317-319.

[19] HADLEY,G.R.: *Transparent boundary condition for beam propagatio*, Opt. Letters, 1991, Vol.16, pp.624-626.

[20] XU,C.L., HUANG, W.P., CHAUDHURI,S.K.: *Efficient and Accurate Vector Mode Calculations by Beam Propagation Method*, IEEE J. of Lightw. Technology, July 1993, Vol.11, No.7, pp.1209-1215.

Received: 01.12.2009.

Modelovanje savremenih fotoničkih komponenti sa složenom geometrijom u transverzalnoj ravni i longitudinalnom pravcu

U radu je dat pregled nekih ključnih dizajnerskih metoda za projektovanje savremenih fotoničkih uređaja i često korišćenih optoelektronskih komponenti. Akcenat rada je na numeričkim simulacionim metodama koje se koriste u integrisanoj fotonici, a zasnovane su na numeričkom rešenju tro-dimenzione vektorske Helmholcove jednačine pri graničnim uslovima otvorenog tipa. Posebna pažnja je usmerena na tzv. metodu prostiranja snopa (BPM) i najpopularniju varijantu ove metode zasnovane na metodi konačnih razlika (FD-BPM). Nedavno razvijene metodologije bazirane na transformaciji koordinata, kao sto je SR-FD-BPM, omogućavaju uspešnu analizu niza fotoničkih uređaja kompleksne geometrije, a posebno onih čiji se oblik ili poprečni presek menja u longitudinalnom pravcu ili u transverzalnoj ravni, sadržeći kose ili zakrivljene razdvojne dielektrične površi. SR-FD-BPM je posebno atraktivna dizajnerska tehnika kada se ima u vidu očekivana kompleksnost fotoničkih integrisanih kola (PIC) u bliskoj budućnosti. U radu su predstavljeni neki ilustrativni primeri projektovanja, bazirani na efikasnim algoritmima transformacije koordinata i SR-FD-BPM-a.

Ključne reči: **optoelektronika, fotonika, prostiranje snopa, integrisana kola, numerička simulacija, metoda konačnih razlika.**

Моделирование современных фотонических составляющих со комплексной геометрией в поперечной плоскости и в продольном направлении

В настоящей работе перечислены некоторые ключевые дизайнерские методы для проектирования современных фотонических оборудований и часто используемых оптоэлектронных составляющих. В работе особенно подчёркнуты цифровые симуляционные методы, пользовавшие в интегрирующей фотонике, обоснованы на цифровом решении трёхразмерного векторного уравнения Гельмгольца при предельным условиям открытого типа. Особое внимание направлено к так называемому методу распространения луча (БРМ) и к самому популярному варианту этого метода, обоснованного на методе конечных разниц (FD-BPM).

Недавно развитые методологии, обоснованы на трансформации координат, какая SR-FD-BPM, обеспечивают успешный анализ целой последовательности фотонических оборудований комплексной геометрии, а особенно тех чьи формы или поперечное сечение меняются в продольном направлении или в поперечной плоскости, а содержат косые или наклонные раздваивающие диэлектрические поверхности. Особенно привлекательной дизайнерской техникой является SR-FD-BPM, если учитывается ожидающая комплексность фотонических интегрирующих схем (PIC) в близком будущем. В работе представлены некоторые пояснительные примеры проектирования, обоснованы на эффективных алгоритмах трансформации координат и SR-FD-BPM.

Ключевые слова: **оптоэлектроника, фотоника, распространение луча, интегрирующие схемы, цифровая симуляция, метод конечных элементов.**

Modélisation des composantes photoniques modernes à géométrie complexe sur le plan transversal et dans le sens longitudinal

Dans ce papier on a donné un aperçu des méthodes clés pour l'élaboration des projets pour les appareils photoniques modernes et pour les composantes optiques électroniques qui sont souvent utilisés. L'accent principal du travail est mis sur les méthodes numériques de simulation employées dans la photonique intégrée et qu sont souvent basées sur la solution numérique de l'équation vectorielle tri-dimensionelle de Helmholtz aux limites du type ouvert. L'attention particulière est portée sur la méthode de la propagation du rayon (BPM) et la version la plus populaire de cette méthode, basée sur la méthode des différences finies(FD – BPM). Les méthodologies développées récemment, basées sur la transformation des coordonnées, telles que SR-FD-BPM , permettent une analyse réussie des séries des appareils photoniques de géométrie complexe, en particulier ceux dont la forme ou l'intersection transversale change dans le sens longitudinal ou sur la plan transversal, comportant des interfaces obliques ou courbées. SR-FD-BPM est une technique de dessin très attrayante notamment en ce qui concerne la complexité attendue des circuits intégrateurs photoniques (PIC) dans le proche avenir. On a présenté aussi les exemples illustratifs des élaborations des projets, basés sur les algorithmes efficaces de la transformation des coordonnées et des SD-FD-BPM.

***Mots clés*: optique électronique, photonique, propagation du rayon, circuits intégrateurs, simulation numérique, méthode des éléments finis.**